Comparison of ACO-OFDM, DCO-OFDM and ADO-OFDM in IM/DD Systems

Sarangi Devasmitha Dissanayake, *Student Member, IEEE*, and Jean Armstrong, *Senior Member, IEEE*

***Abstract*—In this paper, three forms of orthogonal frequency division multiplexing (OFDM) designed for intensity modulated/direct detection (IM/DD) optical systems are compared. These are asymmetrically clipped optical OFDM (ACO-OFDM), DC biased optical OFDM (DCO-OFDM) and asymmetrically clipped DC biased optical OFDM (ADO-OFDM). ADO-OFDM is a new technique that combines aspects of ACO-OFDM and DCO-OFDM by simultaneously transmitting ACO-OFDM on the odd subcarriers and DCO-OFDM on the even subcarriers. The odd subcarriers are demodulated as in a conventional ACO-OFDM receiver and the even subcarriers are demodulated using a form of interference cancellation. ADO-OFDM is shown to be more optically power efficient than conventional ACO-OFDM and DCO-OFDM, for some bit rate/normalized bandwidths. It is also shown that by varying the proportion of optical power on the ACO-OFDM component, the DC bias level of DCO-OFDM and the constellations sent on the odd and even subcarriers, the optical power efficiency of ADO-OFDM can be changed.**

***Index Terms*—ACO-OFDM, ADO-OFDM, DCO-OFDM, IM/DD, optical systems.**

I. Introduction

ORTHOGONAL FREQUENCY DIVISION MULTIPLEXING (OFDM) is extensively used in wired and wireless broadband communication systems due to its resistance to inter symbol interference (ISI) caused by a dispersive channel. OFDM has the added advantage of requiring a simple one tap equalizer at the receiver. OFDM is now increasingly being considered as a modulation technique for optical systems [1]–[3], it has better optical power efficiency than conventional modulation schemes such as on-off-keying (OOK) and pulse position modulation (PPM). In conventional OFDM, the transmitted signals are bipolar and complex, but bipolar signals cannot be transmitted in an intensity modulated/direct detection (IM/DD) optical wireless system, because the intensity of light cannot be negative. OFDM signals designed for IM/DD systems must therefore be real and non-negative. There are several different forms of OFDM for IM/DD systems: asymmetrically clipped optical OFDM (ACO-OFDM) [4], DC biased optical OFDM (DCO-OFDM) [5], and other forms based on ACO-OFDM and DCO-OFDM [6], [7].

Manuscript received May 28, 2012; revised December 18, 2012 and January 09, 2013; accepted January 10, 2013. Date of publication January 21, 2013; date of current version February 06, 2013. This work was supported under an Australian Research Council's (ARC) Discovery funding scheme (DP 1094218).

The authors are with Monash University, Electrical and Computer Systems Engineering, Clayton, Victoria 3800, Australia (e-mail: Sarangi.Dissanayake@monash.edu; Jean.Armstrong@eng.monash.edu.au).

Color versions of one or more of the figures in this paper are available online at http://ieeexplore.ieee.org.

Digital Object Identifier 10.1109/JLT.2013.2241731

In ACO-OFDM, the transmitted signal is made positive, by clipping the original bipolar OFDM signal at zero and transmitting only the positive parts. In DCO-OFDM, a DC bias is added to the signal to make it positive. In ACO-OFDM only the odd subcarriers transmit data symbols, whereas in DCO-OFDM all the subcarriers carry data symbols. DCO-OFDM is less efficient than ACO-OFDM in terms of average optical power for constellations such as 4-QAM, 16-QAM, 64-QAM and 256-QAM [2]. But for larger constellations, such as 1024 QAM and 4096 QAM, DCO-OFDM is more efficient [2]. This is because the DC bias used in DCO-OFDM is inefficient in terms of optical power, while the use of only half of the subcarriers to carry data in ACO-OFDM is inefficient in terms of bandwidth. For small constellations, the first effect is more important and ACO-OFDM gives better overall performance, but for larger constellations, the second effect dominates and DCO-OFDM gives better performance. These effects are explained in more detail in Section II-C.

A number of ways of improving the optical efficiency of OFDM for IM/DD systems have recently been proposed. In [8], a spectrally factorized optical OFDM method which shows a gain of 0.5 dB in optical power over ACO-OFDM at a bit error rate (BER) of is described. In [6], a noise cancellation method is discussed, where the anti-symmetry of the time samples of ACO-OFDM is used to identify which samples of the received signal are most likely to be due to the addition of noise. These samples are then set to zero. A maximum gain of 3 dB in optical power can be achieved with this method. In [9], a diversity combining system for ACO-OFDM is presented, where, after non-linear processing, the signal from the received even subcarriers is combined with the signal from the received odd subcarriers. In conventional ACO-OFDM, the even subcarriers are discarded and only the odd subcarriers are demodulated. The system in [9] can achieve a gain of up to 3 dB in electrical power. However, it is vulnerable to the DC offset which may result from low frequency interference and environmental noise [10]. Two new techniques are described in [10] to reduce the sensitivity to DC offset of diversity combined ACO-OFDM. In [11], the systems in [6] and [9] are combined, and it is shown that no additional performance gain results from the combining of the two systems.

In [12], a new system, developed by the authors, called asymmetrically clipped DC biased optical OFDM (ADO-OFDM) was described and simulation results presented. This paper extends this work and compares the performance of ADO-OFDM with ACO-OFDM and DCO-OFDM. The statistical properties of the signals are analyzed in detail. Extensive simulation results show the effect of varying the constellation sizes, the

clipping level on the DCO-OFDM component, and the proportion of the power allocated to the ACO-OFDM component.

In ADO-OFDM, ACO-OFDM is used on the odd subcarriers and DCO-OFDM is used on the even subcarriers. We will show that this combines the advantages of ACO-OFDM and DCO-OFDM; because all of the subcarriers are used to carry data, the bandwidth efficiency is better than ACO-OFDM, and because the more power efficient ACO-OFDM is used on half of the subcarriers, the overall optical power efficiency is better than DCO-OFDM. The ACO-OFDM component is demodulated as in a conventional ACO-OFDM receiver while the DCO-OFDM component is demodulated using an interference cancellation method.

The rest of the paper is organized as follows. In Section II, the three systems, ACO-OFDM, DCO-OFDM and ADO-OFDM systems are analyzed in terms of their probability density function (PDF), optical power and electrical power. A detailed comparison of the performance of ACO-OFDM and DCO-OFDM is provided in Section II-C. This forms the basis for the explanation of the properties of ADO-OFDM in the following sections. In Section III, simulation results and a discussion of the optical power efficiency of ADO-OFDM are shown. Also, the performance of ADO-OFDM is compared with ACO-OFDM and DCO-OFDM schemes. The paper concludes in Section IV.

II. Analysis of Direct Detection OFDM Schemes

This section describes the DCO-OFDM, ACO-OFDM and ADO-OFDM systems in detail.

A. DCO-OFDM

A DCO-OFDM transmitter is shown in Fig. 1. The complex data signal, $\mathbf{X} = [X_0, X_1, X_2, \cdots, X_{N-1}]$, is input into the inverse fast Fourier transform (IFFT). $\mathbf{X}$ is constrained to have Hermitian symmetry, as defined below,

$$X_m = X^*_{N-m} \quad \text{for} \quad 0 < m < \frac{N}{2}, \tag{1}$$

and the two components X_0 and $X_{N/2}$ are set to zero, i.e. $X_0 = X_{N/2} = 0$. Because of the Hermitian symmetry of the input, the output signal of the IFFT, $\mathbf{x}$, is real not complex. Throughout this paper, we use upper case to represent a signal in the discrete frequency domain and lower case to represent the corresponding discrete time domain signal. The k^{th} time domain sample of $\mathbf{x}$, x_k, is given by

$$x_k = \frac{1}{N} \sum_{m=0}^{N-1} X_m \exp\left(\frac{j2\pi km}{N}\right), \tag{2}$$

where N is the number of points on the IFFT and X_m is the m^{th} subcarrier of signal $\mathbf{X}$. Due to the Hermitian symmetry and $X_0 = X_{N/2} = 0$, the number of unique data carrying subcarriers present in DCO-OFDM is $(N/2) - 1$. Signal $\mathbf{x}$ is then converted from parallel to serial (P/S), a cyclic prefix (CP) is appended, the resulting signal is digital to analog (D/A) converted and low pass filtered resulting in $x(t)$. In this paper, an ideal low pass filter (LPF) is assumed.

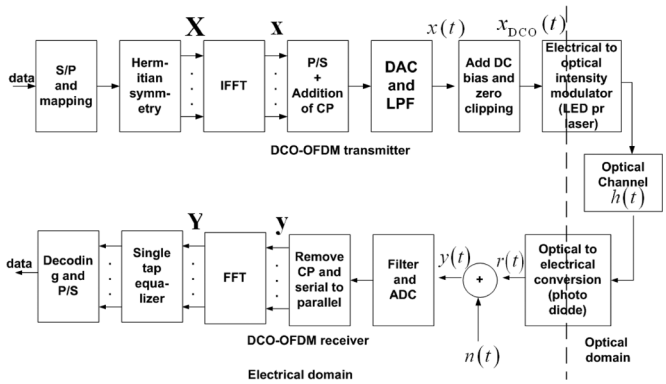

Fig. 1. DCO-OFDM system.

For large N values, the signal $x(t)$ can be modeled as a Gaussian random variable with a zero mean and a variance of $\sigma^2_{\text{D}} = E\{x_k^2\}$. Next a suitable DC bias is added to $x(t)$ and any remaining negative peaks are clipped resulting in signal $x_{\text{DCO}}(t)$. Because OFDM signals have a very high peak-to-average power ratio, a very high bias is required to eliminate all negative peaks [2]. If a large DC bias is used, the optical energy-per-bit to single sided noise power spectral density, $E_{\text{b(opt)}}/N_0$, becomes very large, thereby making the scheme inefficient in terms of optical power. Instead, a moderate bias is normally used, and the remaining negative peaks are clipped, resulting in clipping noise. In typical DCO-OFDM systems both odd and even subcarriers carry data symbols and the clipping noise affects all the subcarriers. The DC bias level is denoted by B_{DC}. B_{DC} is set relative to the standard deviation of $x(t)$ [5],

$$B_{\text{DC}} = \mu\sqrt{E\left\{x(t)^2\right\}}, \tag{3}$$

where μ is a proportionality constant. B_{DC} is defined as a bias of $10\log_{10}(\mu^2+1)$ dB. Any negative peak which remains after the addition of B_{DC} is clipped at zero. Signal $x_{\text{DCO}}(t)$ is then input to an optical modulator. In this paper, we assume an ideal optical modulator, so that the intensity of the output optical signal is directly proportional to the input electrical current. The resulting signal is transmitted across a flat channel. Shot noise which affects the signal is modeled as additive white Gaussian noise (AWGN), $n(t)$, added in the electrical domain [5].

At the receiver, the received signal is first converted from an optical signal to an electrical signal using a photodiode. The processing after this point is the same as a conventional OFDM receiver [13].

The PDF of $x_{\text{DCO}}(t)$ is a clipped Gaussian distribution given by [14], [15]

$$f_{x_{\text{DCO}}(t)}(v) = \frac{1}{\sqrt{2\pi}\sigma_{\text{D}}} \exp\left(\frac{-(v - B_{DC})^2}{2\sigma^2_{\text{D}}}\right) u(v) + Q\left(\frac{B_{DC}}{\sigma_{\text{D}}}\right)\delta(v), \tag{4}$$

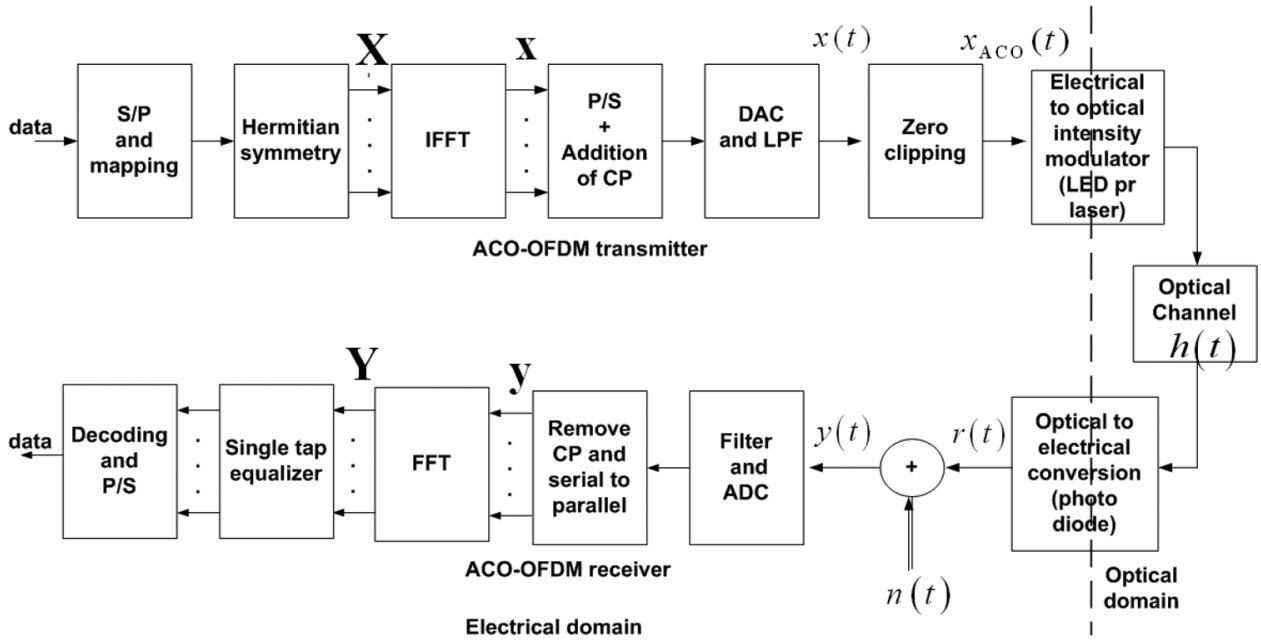

Fig. 2. ACO-OFDM system.

where $u(v)$ is a unit step function and $\delta(v)$ is the Dirac delta function. The optical power of DCO-OFDM, $P_{\text{opt,DCO}}$, is given by,

$$P_{\text{opt,DCO}} = E\{x_{\text{DCO}}(t)\} = \int_0^\infty v f_{x_{\text{DCO}}(t)}(v)dv$$
$$= \frac{\sigma_{\text{D}}}{2\pi}\exp\left(\frac{-B_{\text{DC}}^2}{2\sigma_{\text{D}}^2}\right) + B_{\text{DC}}\left(1 - Q\left(\frac{B_{\text{DC}}}{\sigma_{\text{D}}}\right)\right), \quad (5)$$

where

$$Q(\xi) = \frac{1}{\sqrt{2\pi}}\int_\xi^\infty \exp\left(-\frac{u^2}{2}\right)du. \quad (6)$$

The electrical power of DCO-OFDM, $P_{\text{elec,DCO}}$, is given by [14], [15]

$$P_{\text{elec,DCO}} = E\left\{x_{\text{DCO}}^2(t)\right\} = \int_0^\infty v^2 f_{x_{\text{DCO}}(t)}(v)dv$$
$$= \left(\sigma_{\text{D}}^2 + B_{\text{DC}}^2\right)\left(1 - Q\left(\frac{B_{\text{DC}}}{\sigma_{\text{D}}}\right)\right)$$
$$+ \frac{\sigma_{\text{D}} B_{\text{DC}}}{\sqrt{2\pi}}\exp\left(\frac{-B_{\text{DC}}^2}{2\sigma_{\text{D}}^2}\right). \quad (7)$$

B. ACO-OFDM

In ACO-OFDM, only the odd subcarriers carry data symbols, while the even subcarriers form a bias signal which ensures that the transmitted OFDM signal meets the non-negativity requirement [2].

Fig. 2 shows an ACO-OFDM system. The input signal to the IFFT, $\mathbf{X}$, comprises only odd components such that $\mathbf{X} = [0, X_1, 0, X_3, \cdots, X_{N-1}]$. Also, the elements of the vector $\mathbf{X}$ are constrained to have Hermitian symmetry as defined in (1). The resulting time domain signal, $\mathbf{x}$, is real and has the anti symmetry property as defined below [6],

$$x_k = -x_{k+\frac{N}{2}} \quad \text{for} \quad 0 < k < \frac{N}{2}. \quad (8)$$

The front-end of the ACO-OFDM transmitter is similar to a DCO-OFDM transmitter where $\mathbf{x}$ is first serialized and a CP is appended to it. Then $\mathbf{x}$ is D/A converted and sent across an ideal LPF resulting in the signal, $x(t)$. As negative samples cannot be transmitted in an IM/DD system, $x(t)$ is clipped at zero which results in the ACO-OFDM signal, $x_{\text{ACO}}(t)$. As a result of the anti-symmetry of $\mathbf{x}$ [6], clipping does not result in any loss of information. Due to the ACO-OFDM clipping the signal on the odd elements of $X_{\text{ACO},m}$ becomes $X_m/2$, where $X_{\text{ACO},m}$ is the m^{th} subcarrier of the discrete frequency transform vector of $x_{\text{ACO}}(t)$. While a new noise like interference signal appears on the even subcarriers [4]. $x_{\text{ACO}}(t)$ is then input to an ideal optical modulator and the resulting signal transmitted across a flat AWGN channel. The processing in the receiver is similar to a DCO-OFDM receiver, except that in ACO-OFDM only the odd subcarriers are demodulated, as only they carry the data symbols.

The PDF of $x_{\text{ACO}}(t)$ is first derived to obtain the optical and electrical power of the ACO-OFDM signal. Using the central limit theorem, it can be shown that the PDF of $x_{\text{ACO}}(t)$ is given by [14], [16]

$$f_{x_{\text{ACO}}(t)}(w) = \frac{1}{\sqrt{2\pi}\sigma_{\text{A}}}\exp\left(\frac{-w^2}{2\sigma_{\text{A}}^2}\right)u(w) + \frac{1}{2}\delta(w), \quad (9)$$

where σ_{A} is the standard deviation of the unclipped signal [16], therefore $\sigma_{\text{A}} = E\{x_k^2\}$. The optical power of ACO-OFDM, $P_{\text{opt,ACO}}$, is given by

$$P_{\text{opt,ACO}} = E\left\{x_{\text{ACO}}(t)\right\} = \int_0^\infty w f_{x_{\text{ACO}}(t)}(w)dw = \frac{\sigma_{\text{A}}}{\sqrt{2\pi}}. \quad (10)$$

The electrical power of the ACO-OFDM, $P_{\mathrm{elec,ACO}}$, is given by

$$P_{\mathrm{elec,ACO}} = E\left\{x_{\mathrm{ACO}}^2(t)\right\} = \int_0^\infty w^2 f_{x_{\mathrm{ACO}}(t)}(w)dw = \frac{\sigma_{\mathrm{A}}^2}{2}. \tag{11}$$

The relationship between (10) and (11) is

$$E\left\{x_{\mathrm{ACO}}(t)\right\} = \frac{\sqrt{E\left\{x_{\mathrm{ACO}}^2(t)\right\}}}{\sqrt{\pi}}. \tag{12}$$

The ratio of $E\{x_{\mathrm{ACO}}(t)\}$ and $E\{x_{\mathrm{ACO}}^2(t)\}$ depends on the level of optical power on $P_{\mathrm{opt,ACO}}$. For the case where $P_{\mathrm{opt,ACO}} = 1$ [2],

$$\frac{E_{\mathrm{b(opt)}}}{N_0} = \frac{1}{\pi}\frac{E_{\mathrm{b(elec)}}}{N_0}. \tag{13}$$

$E_{\mathrm{b(opt)}}/N_0$ of ACO-OFDM is given by $E\{x_{\mathrm{ACO}}(t)\}/b_{\mathrm{ACO}}N_0$ and electrical energy-per-bit to single sided noise power spectral density, $E_{\mathrm{b(elec)}}/N_0$, of ACO-OFDM is given by $E\{x_{\mathrm{ACO}}^2(t)\}/b_{\mathrm{ACO}}N_0$. b_{ACO} is the bit rate of ACO-OFDM.

C. Performance Comparison of ACO-OFDM and DCO-OFDM

In this section the performances of ACO-OFDM and DCO-OFDM are compared.

In radio frequency (RF) systems, graphs of $E_{\mathrm{b(elec)}}/N_0$, against bit error rate (BER) graphs are normally used to compare different modulation schemes. Unfortunately there is no simple way to measure the performance of different modulation schemes in IM/DD systems. This is because in IM/DD systems, the BER depends on the signal to noise ratio (SNR) of the *electrical* signal while the limiting factor is the amount of average *optical* power that can be transmitted.

In earlier papers, the performance comparison was done in terms of normalized $E_{\mathrm{b(opt)}}/N_0$ and *normalized bandwidth/bit rate* [2], [17]. Normalized $E_{\mathrm{b(opt)}}/N_0$ is the value when the average optical power is set to unity. In this paper a different approach is employed, where the variation of normalized $E_{\mathrm{b(opt)}}/N_0$ with *bit rate/normalized bandwidth* is used. This demonstrates the properties of ACO-OFDM, DCO-OFDM and ADO-OFDM more clearly.

Throughout this paper the average optical power of the total received power for all the modulation schemes is set to unity. The required normalized $E_{\mathrm{b(opt)}}/N_0$ for a BER of 10^{-3}, defined as $\langle E_{\mathrm{b(opt)}}/N_0\rangle_{\mathrm{BER}}$, is used in the simulations.

Following [5] and [2], the modulation bandwidth is defined as the position of the first spectral null. When modulation bandwidth is normalized relative to on-off keying (OOK) of the same data rate, normalized bandwidth is obtained. For ACO-OFDM and DCO-OFDM the first null occurs at the a normalized frequency of $1 + 2/N$. Therefore, the bit rate/normalized bandwidth of ACO-OFDM is $\log_2 M_{\mathrm{ACO}}/2(1+2/N)$, where M_{ACO} is the QAM constellation size of ACO-OFDM. The factor of half results from the fact that only half of the subcarriers carry data symbols in ACO-OFDM. The bit rate/normalized bandwidth for DCO-OFDM is $\log_2 M_{\mathrm{DCO}}/(1+2/N)$, where M_{DCO} is the QAM constellation size of DCO-OFDM.

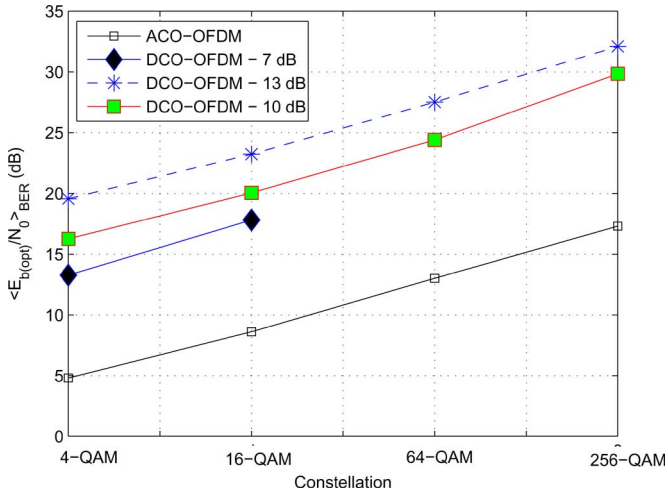

Fig. 3. $\langle E_{\mathrm{b(opt)}}/N_0\rangle_{\mathrm{BER}}$ against different constellations for ACO-OFDM and DCO-OFDM with 7 dB, 10 dB and 13 dB bias levels.

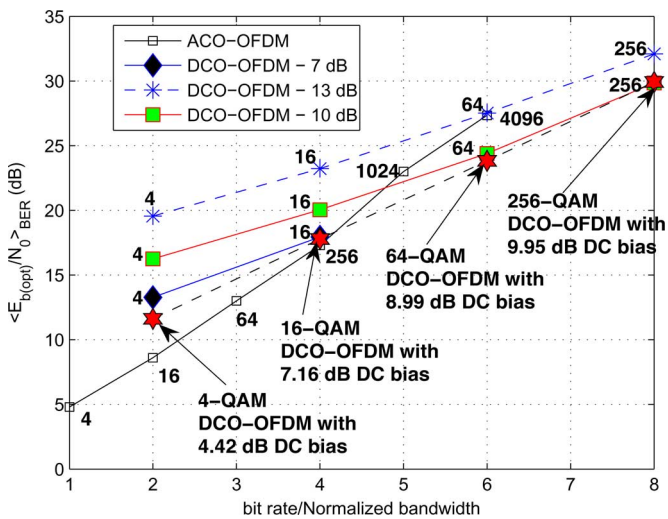

Fig. 4. $\langle E_{\mathrm{b(opt)}}/N_0\rangle_{\mathrm{BER}}$ against bit rate/normalized bandwidth for ACO-OFDM 4-QAM, 16-QAM, 64-QAM, 256-QAM, 1024-QAM and 4096-QAM constellations and DCO-OFDM 4-QAM, 16-QAM, 64-QAM and 256-QAM constellations with 7 dB, 10 dB and 13 dB bias levels. Minimum possible $\langle E_{\mathrm{b(opt)}}/N_0\rangle_{\mathrm{BER}}$ for each constellation of DCO-OFDM along with the Bias level.

For DCO-OFDM $E_{\mathrm{b(opt)}}/N_0$ is given by $E\{x_{\mathrm{DCO}}(t)\}/b_{\mathrm{DCO}}N_0$, where the bit rate of DCO-OFDM is given by b_{DCO}.

Fig. 3 and Fig. 4 plot $\langle E_{\mathrm{b(opt)}}/N_0\rangle_{\mathrm{BER}}$ against different constellations and bit rate/normalized bandwidth respectively, for ACO-OFDM and DCO-OFDM with a 7 dB, 10 dB and 13 dB bias. In Fig. 4, the values of the minimum possible $\langle E_{\mathrm{b(opt)}}/N_0\rangle_{\mathrm{BER}}$ for each constellation of DCO-OFDM are also shown, along with the bias required to achieve this minimum. Fig. 3 makes clear the effect of increased constellation sizes on $\langle E_{\mathrm{b(opt)}}/N_0\rangle_{\mathrm{BER}}$, while Fig. 4 shows how $\langle E_{\mathrm{b(opt)}}/N_0\rangle_{\mathrm{BER}}$ varies with bit rate. From Fig. 3, it is observed that ACO-OFDM requires the lowest $\langle E_{\mathrm{b(opt)}}/N_0\rangle_{\mathrm{BER}}$ for 4-QAM, 16-QAM, 64-QAM and 256-QAM constellations, while DCO-OFDM requires higher $\langle E_{\mathrm{b(opt)}}/N_0\rangle_{\mathrm{BER}}$ due to the addition of DC bias. When the DC bias added to the

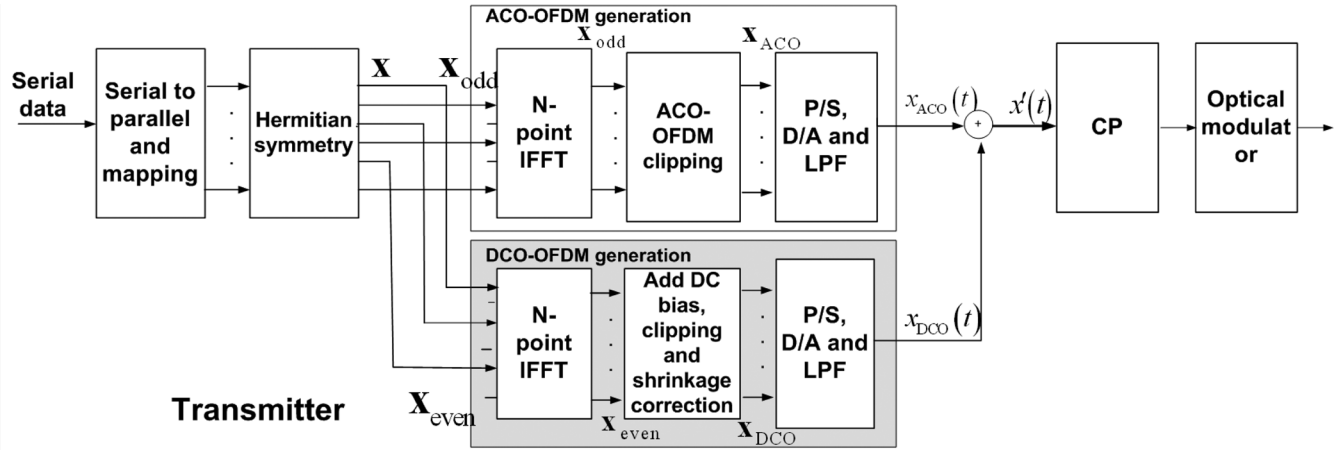

Fig. 5. ADO-OFDM transmitter.

DCO-OFDM is low, for example when it is 7 dB, only 4-QAM and 16-QAM can be demodulated with BER of 10^{-3} or less. While with a 13 dB DC bias, 4-QAM, 16-QAM, 64-QAM and 256-QAM constellations can be successfully demodulated. Constellations such as 64-QAM and 256-QAM result in very high bit error rates for a 7 dB bias due to the high clipping noise [2]. Another important observation is that all the curves in Fig. 3 are parallel to each other, which means that the rate of increase of $\langle E_{\mathrm{b(opt)}}/N_0\rangle_{\mathrm{BER}}$ is the same for both ACO-OFDM and DCO-OFDM. Due to ACO-OFDM transmitting data symbols on only half of its subcarriers, the bit rate of ACO-OFDM is half that of DCO-OFDM for a given constellation. Therefore, in Fig. 4, a 16-QAM ACO-OFDM constellation is comparable with that of 4-QAM DCO-OFDM constellation. Hence, as shown in Fig. 4, the rate of increase of the required $\langle E_{\mathrm{b(opt)}}/N_0\rangle_{\mathrm{BER}}$ is faster for ACO-OFDM than DCO-OFDM. This is why ACO-OFDM becomes less efficient in terms of optical power than DCO-OFDM for large constellations such as 1024-QAM and 4096-QAM.

Fig. 4 also shows that for DCO-OFDM the minimum bias level for a given BER does not necessarily result in the minimum $\langle E_{\mathrm{b(opt)}}/N_0\rangle_{\mathrm{BER}}$. This is because, if the bias is too low, the level of clipping noise increases and the level of AWGN must be very low to achieve the target BER.

D. ADO-OFDM

In ADO-OFDM, ACO-OFDM and DCO-OFDM are transmitted simultaneously. ACO-OFDM is transmitted on the odd subcarriers and DCO-OFDM is transmitted on the even subcarriers. The odd subcarriers are demodulated as in a conventional ACO-OFDM receiver [17] and the even subcarriers are demodulated after an interference cancellation process [12].

ADO-OFDM Transmitter: Fig. 5 shows the block diagram of an ADO-OFDM transmitter. The upper path in the transmitter generates the ACO-OFDM signals and the lower path generates the DCO-OFDM signals. The signal processing of the ACO-OFDM path is very similar to that of a conventional ACO-OFDM transmitter [17]. The input data vector, $\mathbf{X}$, which is constrained to have Hermitian symmetry, is divided into odd and even components, $\mathbf{X}_{\mathrm{odd}}$ and $\mathbf{X}_{\mathrm{even}}$, where $\mathbf{X}_{\mathrm{odd}} = [0, X_1, 0, X_3, 0, \ldots, 0, X_{N-1}]$ and $\mathbf{X}_{\mathrm{even}} = [X_0, 0X_2, 0, \ldots, X_{N-2}, 0]$. As the elements of $\mathbf{X}$ have Hermitian symmetry, the elements of $\mathbf{X}_{\mathrm{odd}}$ and $\mathbf{X}_{\mathrm{even}}$ will also have Hermitian symmetry. $\mathbf{X}_{\mathrm{odd}}$ and $\mathbf{X}_{\mathrm{even}}$ are then input to two separate IFFT blocks to produce $\mathbf{x}_{\mathrm{odd}}$ and $\mathbf{x}_{\mathrm{even}}$ respectively, where $\mathbf{x}_{\mathrm{odd}} = [\mathbf{x}_{\mathrm{odd},0}, \mathbf{x}_{\mathrm{odd},1}, \ldots, \mathbf{x}_{\mathrm{odd},N-1}]$ and $\mathbf{x}_{\mathrm{even}} = [\mathbf{x}_{\mathrm{even},0}, \mathbf{x}_{\mathrm{even},1}, \ldots, \mathbf{x}_{\mathrm{even},N-1}]$. The resulting $\mathbf{x}_{\mathrm{odd}}$ signal is real and bipolar. Next by clipping the negative peaks of $\mathbf{x}_{\mathrm{odd}}$, the ACO-OFDM signal, $\mathbf{x}_{\mathrm{ACO}}$ signal is generated. $\mathbf{x}_{\mathrm{ACO}}$ is as follows;

$$\mathbf{x}_{\mathrm{ACO}} = \frac{1}{2}\mathbf{x}_{\mathrm{odd}} + \mathbf{n}_{\mathrm{ACO}}, \tag{14}$$

where $\mathbf{n}_{\mathrm{ACO}}$ is the ACO-OFDM clipping noise. The Fourier transform of $\mathbf{n}_{\mathrm{ACO}}$ comprises even subcarriers only while the Fourier transform of $\mathbf{x}_{\mathrm{odd}}$ comprises odd subcarriers only [4].

In the DCO-OFDM, the $\mathbf{x}_{\mathrm{DCO}}$ signal is generated by adding a DC-bias to the discrete time domain signal, $\mathbf{x}_{\mathrm{even}}$, and clipping any remaining negative peaks. As $\mathbf{x}_{\mathrm{even}}$ is generated from only the even index subcarriers, it has even symmetry. Therefore,

$$x_{\mathrm{even},k} = x_{\mathrm{even},k+N/2} \quad 0 \le k < \frac{N}{2}. \tag{15}$$

When a DC bias, B_{DC}, is added we have

$$x_{\mathrm{even},k} + B_{\mathrm{DC}} = x_{\mathrm{even},k+N/2} + B_{\mathrm{DC}} \quad 0 \le k < \frac{N}{2}. \tag{16}$$

Therefore, for every negative peak that is clipped for $0 \le k < N/2$, an identical peak is clipped at $k + N/2$. To simplify the analysis we assume that the shrinkage is corrected after clipping and denote the new DC component by B'_{DC}. The DCO-OFDM clipping noise is given by $\mathbf{n}_{\mathrm{DCO}}$ [12]. Therefore, the resulting DCO-OFDM signal is given by

$$\mathbf{x}_{\mathrm{DCO}} = \mathbf{x}_{\mathrm{even}} + \mathbf{n}_{\mathrm{DCO}} + B'_{\mathrm{DC}}, \tag{17}$$

where

$$x_{\mathrm{DCO},k} = x_{\mathrm{DCO},k+N/2} \quad 0 \le k < \frac{N}{2}. \tag{18}$$

Combining (15), (16), (17) and (18) it can be seen that

$$n_{\mathrm{DCO},k} = n_{\mathrm{DCO},k+N/2} \quad 0 \le k < \frac{N}{2}. \tag{19}$$

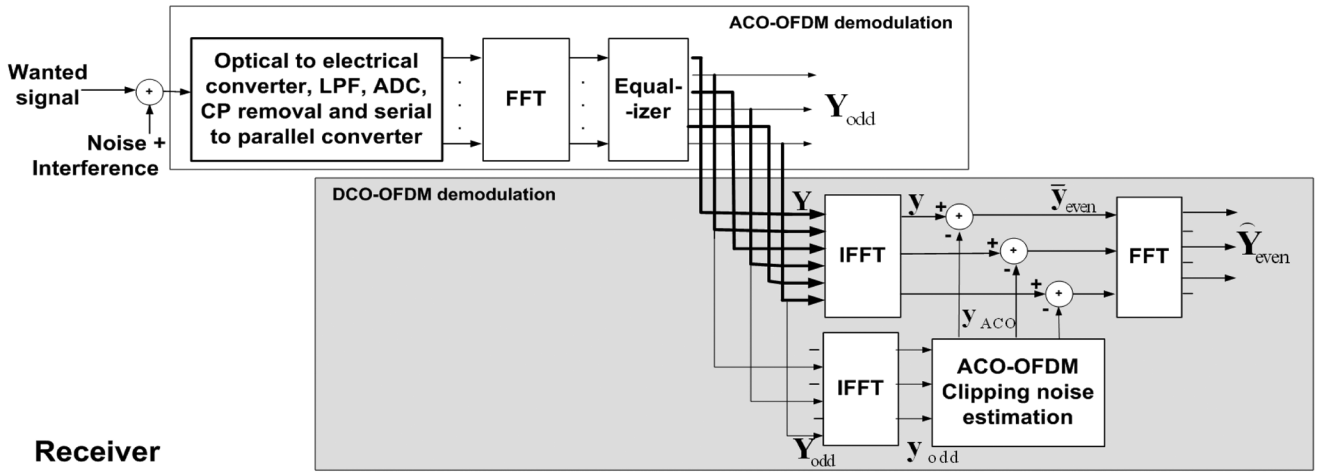

Fig. 6. ADO-OFDM receiver.

Therefore, when the original DCO-OFDM signal consists of only even subcarriers, $\mathbf{n}_{\text{DCO}}$ will affect only the even index subcarriers. This is important as it means that the performance of the ACO-OFDM is not degraded by the DCO-OFDM clipping noise.

Next, the signals, $\mathbf{X}_{\text{ACO}}$ and $\mathbf{X}_{\text{DCO}}$ are serialized, converted from D/A and sent via an ideal LPF resulting in the continuous time domain signal $x_{\text{ACO}}(t)$ and $x_{\text{DCO}}(t)$. Signal $x'(t)$ is generated by adding $x_{\text{ACO}}(t)$ and $x_{\text{DCO}}(t)$ together,

$$x'(t) = x_{\text{ACO}}(t) + x_{\text{DCO}}(t). \tag{20}$$

A CP is appended to $x'(t)$. $x'(t)$ is then sent across an ideal optical modulator.

ADO-OFDM Receiver: An ADO-OFDM receiver is shown in Fig. 6, where there is a separate path to demodulate the ACO-OFDM symbols and another path to demodulate the DCO-OFDM symbols.

A flat channel is assumed with AWGN and perfect equalization at the receiver. To simplify the analysis we consider the AWGN as consisting of separate components due to the odd and even received subcarrier frequencies, $\mathbf{n}_{\text{odd,AWGN}}$ and $\mathbf{n}_{\text{even,AWGN}}$. Because we are considering a flat channel and AWGN, the elements of these two vectors are independent, identically distributed (i.i.d.) Gaussian variables. The resulting signal is

$$\mathbf{y} = \frac{1}{2}\mathbf{x}_{\text{odd}} + \mathbf{n}_{\text{ACO}} + \mathbf{x}_{\text{even}} + \mathbf{n}_{\text{DCO}} + B'_{\text{DC}} + \mathbf{n}_{\text{odd,AWGN}} + \mathbf{n}_{\text{even,AWGN}}, \tag{21}$$

of which only $\mathbf{x}_{\text{odd}}/2$ and $\mathbf{n}_{\text{odd,AWGN}}$ contribute to the odd frequency subcarriers. Therefore,

$$\mathbf{Y}_{\text{odd}} = \frac{1}{2}\mathbf{X}_{\text{odd}} + \mathbf{N}_{\text{odd,AWGN}}, \tag{22}$$

where the data transmitted on the odd frequency subcarriers using ACO-OFDM can be recovered from the corresponding subcarriers at the receiver. Taking the FFT of (21) gives

$$\mathbf{Y} = \frac{1}{2}\mathbf{X}_{\text{odd}} + \mathbf{N}_{\text{ACO}} + \mathbf{X}_{\text{even}} + \mathbf{N}_{\text{DCO}} + B'_{\text{DC}} + \mathbf{N}_{\text{odd,AWGN}} + \mathbf{N}_{\text{even,AWGN}}. \tag{23}$$

Before demodulating the DCO-OFDM signals, we need to subtract the interfering ACO-OFDM signal. This is achieved by generating a local estimate of the ACO-OFDM signal and subtracting it from the received signal. To achieve this $\mathbf{Y}_{\text{odd}}$ is input to an IFFT to generate $\mathbf{y}_{\text{odd}}$, then multiplied by two to generate an estimate of $\mathbf{x}_{\text{odd}}$ which is clipped at zero to give $\mathbf{y}_{\text{ACO}}$ where

$$\mathbf{y}_{\text{ACO}} = \mathbf{x}_{\text{ACO}} + \mathbf{n}_{\text{ACO even,AWGN}} + \mathbf{n}_{\text{ACO odd,AWGN}}. \tag{24}$$

This estimation process results in a noise power component in the even subcarriers, $\mathbf{n}_{\text{ACO even,AWGN}}$, and a noise power component in the odd subcarriers, $\mathbf{n}_{\text{ACO odd,AWGN}}$. Because ACO clipping results in equal total power in odd and even subcarriers [4], $\mathbf{n}_{\text{ACO odd,AWGN}}$ and $\mathbf{n}_{\text{ACO even,AWGN}}$ also have equal average noise power. The estimated ACO-OFDM signal, $\mathbf{y}_{\text{ACO}}$, is then subtracted from the combined signal, $\mathbf{y}$, and the resultant signal, $\bar{\mathbf{y}}_{\text{even}}$, input to an FFT. The resulting even subcarriers $\widehat{\mathbf{Y}}_{\text{even}}$ are used to estimate the DCO-OFDM signal. Combining (22), (23) and (24) gives

$$\widehat{\mathbf{Y}}_{\text{even}} = \mathbf{X}_{\text{even}} + \mathbf{N}_{\text{DCO}} + K'_{\text{DC}} + \mathbf{N}_{\text{ACO even,AWGN}} + \mathbf{N}_{\text{even,AWGN}}. \tag{25}$$

It can be seen that, $\widehat{\mathbf{Y}}_{\text{even}}$ provides a noisy estimate of the transmitted DCO-OFDM signal. There are three sources of noise, the original DCO clipping noise, the AWGN added in the channel to the even subcarriers and an extra noise component caused by the use of a noisy estimate of the ACO-OFDM signal in the interference cancellation process. As $\mathbf{N}_{\text{ACO even,AWGN}}$ and $\mathbf{N}_{\text{even,AWGN}}$ are i.i.d. Gaussian variables, the effective AWGN power is doubled for the DCO-OFDM component. However, because there is no clipping noise on the odd subcarriers, the clipping noise is not doubled by the interference cancellation process.

E. The PDF of ADO-OFDM

In this section the PDF, the optical power and the electrical power of the transmitted ADO-OFDM signal are analytically derived.

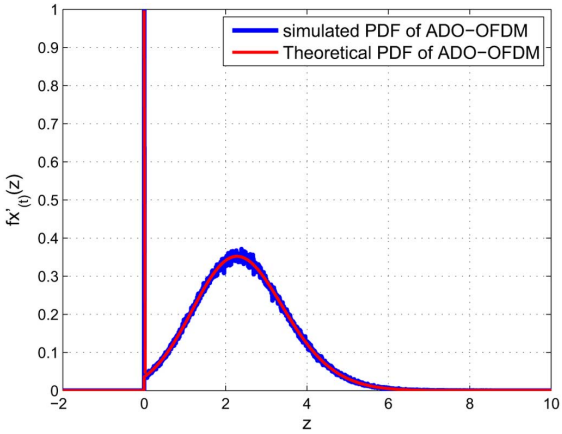

Fig. 7. Simulated and theoretical PDF of ADO-OFDM.

The PDF of $x_{\mathrm{DCO}}(t)$ is given by (4) where $\sigma_{\mathrm{D}} = E\{x^2_{\mathrm{even},k}\}$ and the PDF of $x_{\mathrm{ACO}}(t)$ is given by (9) where $\sigma_{\mathrm{A}} = E\{x^2_{\mathrm{odd},k}\}$. Due to the relationship in (20), the PDF of $x'(t)$ is derived by convolving the PDF of ACO-OFDM and the PDF of DCO-OFDM. Therefore, the PDF of $x'(t)$ is

$$f_{x'(t)}(z) = \int_{-\infty}^{\infty} f_{x_{\mathrm{DCO}}(t)}(z-\lambda) f_{x_{\mathrm{ACO}}(t)}(\lambda) d\lambda. \tag{26}$$

Substituting (9) and (4) in (26) gives

$$\begin{aligned} f_{x'(t)}(z) = \int_0^{\infty} & \left(\frac{1}{\sqrt{2\pi}\sigma_{\mathrm{D}}} \exp\left(\frac{-(\lambda - B_{\mathrm{DC}})^2}{2\sigma_{\mathrm{D}}^2} \right) u(\lambda) \right. \\ & \left. + Q\left(\frac{B_{\mathrm{DC}}}{\sigma_{\mathrm{D}}} \right) \delta(\lambda) \right) \\ & \times \left(\frac{1}{2}\delta(z-\lambda) \right. \\ & \left. + \frac{1}{\sqrt{2\pi}\sigma_{\mathrm{A}}} \exp\left(\frac{-(z-\lambda)^2}{2\sigma_{\mathrm{A}}^2} \right) u(z-\lambda) \right) d\lambda. \end{aligned} \tag{27}$$

Equation (27) can be simplified to

$$\begin{aligned} f_{x'(t)}(z) = & \frac{1}{\sqrt{2\pi\left(\sigma_{\mathrm{D}}^2 + \sigma_{\mathrm{A}}^2\right)}} \exp\left(\frac{-(z - B_{\mathrm{DC}})^2}{2\left(\sigma_{\mathrm{D}}^2 + \sigma_{\mathrm{A}}^2\right)} \right) \\ & \times \left\{ Q\left(\frac{z\sigma_{\mathrm{D}}^2 + B_{\mathrm{DC}}\sigma_{\mathrm{A}}^2}{-\sqrt{\sigma_{\mathrm{D}}^2\sigma_{\mathrm{A}}^2\left(\sigma_{\mathrm{D}}^2 + \sigma_{\mathrm{A}}^2\right)}} \right) \right. \\ & \left. - Q\left(\frac{z\sigma_{\mathrm{A}}^2 - B_{\mathrm{DC}}\sigma_{\mathrm{A}}^2}{\sqrt{\sigma_{\mathrm{D}}^2\sigma_{\mathrm{A}}^2\left(\sigma_{\mathrm{D}}^2 + \sigma_{\mathrm{A}}^2\right)}} \right) \right\} \\ & + \frac{1}{\sqrt{2\pi}\sigma_{\mathrm{A}}} \exp\left[\frac{-z^2}{2\sigma_{\mathrm{A}}^2} \right] Q\left(\frac{B_{\mathrm{DC}}}{\sigma_{\mathrm{D}}} \right) u(z) \\ & + \frac{1}{2\sqrt{2\pi}\sigma_{\mathrm{D}}} \exp\left(\frac{-(z - B_{\mathrm{DC}})^2}{2\sigma_{\mathrm{D}}^2} \right) u(z) \\ & + \frac{1}{2}\delta(z) Q\left(\frac{B_{\mathrm{DC}}}{\sigma_{\mathrm{D}}} \right). \end{aligned} \tag{28}$$

The simplification of (28) is shown in Appendix. The simulated and the theoretical PDFs of ADO-OFDM are shown in Fig. 7 and they both closely follow each other. Hence, the optical power of the ADO-OFDM signal, $P_{\mathrm{opt,ADO}}$, is given by

TABLE I
ADO-OFDM SCHEMES SIMULATED

ADO-OFDM	DC bias level
4-QAM ACO, 16-QAM DCO	3 dB
256-QAM ACO, 4-QAM DCO	7 dB
64-QAM ACO, 16-QAM DCO	7 dB
256-QAM ACO, 16-QAM DCO	7 dB
256-QAM ACO, 16-QAM DCO	10 dB

$$P_{\mathrm{opt,ADO}} = E\{x'(t)\} = \int_0^{\infty} z f_{x'(t)}(z) dz. \tag{29}$$

By substituting (28) in (29) and simplifying we obtain

$$\begin{aligned} E\{x'(t)\} = & \frac{B_{\mathrm{DC}}}{2} - \frac{B_{\mathrm{DC}}}{2} Q\left(\frac{B_{\mathrm{DC}}}{\sigma_{\mathrm{D}}} \right) \\ & + \frac{\sigma_{\mathrm{D}}^2}{2\sqrt{2\pi}} \exp\left(\frac{-B_{\mathrm{DC}}^2}{2\sigma_{\mathrm{D}}^2} \right) + \frac{\sigma_{\mathrm{A}}}{\sqrt{2\pi}} Q\left(\frac{B_{\mathrm{DC}}}{\sigma_{\mathrm{D}}} \right) \\ & + \frac{1}{\sqrt{2\pi}} \left\{ \left(1 - Q\left(\frac{B_{\mathrm{DC}}}{\sigma_{\mathrm{D}}} \right) \right) \sigma_{\mathrm{A}} \right. \\ & \left. + \frac{\sigma_{\mathrm{D}}}{2} \exp\left(\frac{-B_{\mathrm{DC}}^2}{2\sigma_{\mathrm{D}}^2} \right) \right\} + A. \end{aligned} \tag{30}$$

where

$$\begin{aligned} A = & \int_{-B_{\mathrm{DC}}}^{\infty} \frac{B_{\mathrm{DC}}}{\sqrt{2\pi\left(\sigma_{\mathrm{D}}^2 + \sigma_{\mathrm{A}}^2\right)}} \exp\left(\frac{-u^2}{2\left(\sigma_{\mathrm{D}}^2 + \sigma_{\mathrm{A}}^2\right)} \right) \\ & \times \left(Q\left(\frac{\sigma_{\mathrm{D}}^2 u + \left(\sigma_{\mathrm{D}}^2 + \sigma_{\mathrm{A}}^2\right) B_{\mathrm{DC}}}{-\sigma_{\mathrm{A}}\sigma_{\mathrm{D}}\sqrt{\left(\sigma_{\mathrm{D}}^2 + \sigma_{\mathrm{A}}^2\right)}} \right) \right. \\ & \left. - Q\left(\frac{\sigma_{\mathrm{A}} u}{\sigma_{\mathrm{D}}\sqrt{\left(\sigma_{\mathrm{D}}^2 + \sigma_{\mathrm{A}}^2\right)}} \right) \right) du. \end{aligned}$$

No closed form solution exists for A in (30). Therefore, the value of $P_{\mathrm{opt,ADO}}$ was found using numerical integration. Table I shows the values for which simulations were performed. The proportion of optical power on the ACO-OFDM and DCO-OFDM components is set to be 0.5 each. Therefore, the total optical power of the ADO-OFDM signal remains at unity. The simulations confirmed that the theoretical derivation of the optical power of ADO-OFDM shown in (30) is in close agreement with the simulated optical power. Similarly, the electrical power of ADO-OFDM is given by

$$P_{\mathrm{elec,ADO}} = E\{x'(t)^2\} = \int_0^{\infty} z^2 f_{x'(t)}(z) dz, \tag{31}$$

which also has no closed form solution.

III. RESULTS

In this section, simulation results for the optical power efficiency of ADO-OFDM are presented and compared with the optical power of conventional ACO-OFDM and DCO-OFDM. The optical power of ADO-OFDM depends on several factors. These are the proportion of the total optical power allocated to

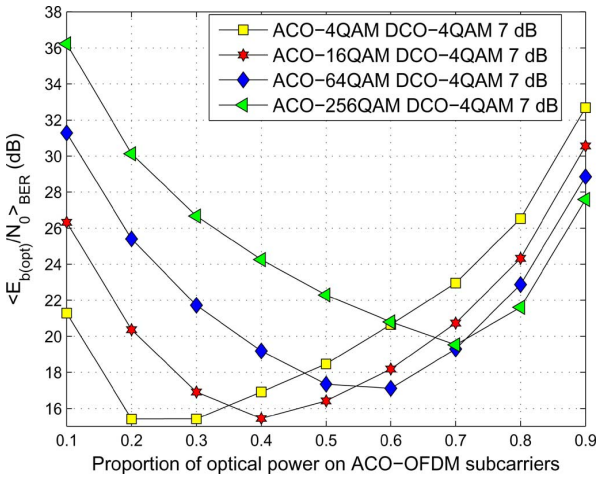

Fig. 8. The variation of $\langle E_{\mathrm{b(opt)}}/N_0\rangle_{\mathrm{BER}}$ with the proportion of optical power on the ACO-OFDM subcarriers, for ADO-OFDM with different constellations on ACO-OFDM and 4-QAM on DCO-OFDM.

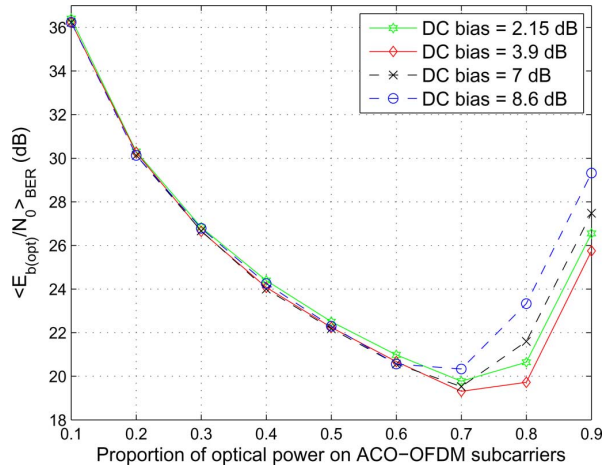

Fig. 9. Variation of $\langle E_{\mathrm{b(opt)}}/N_0\rangle_{\mathrm{BER}}$ with the clipping level for 4-QAM DCO-OFDM and 256-QAM ACO-OFDM.

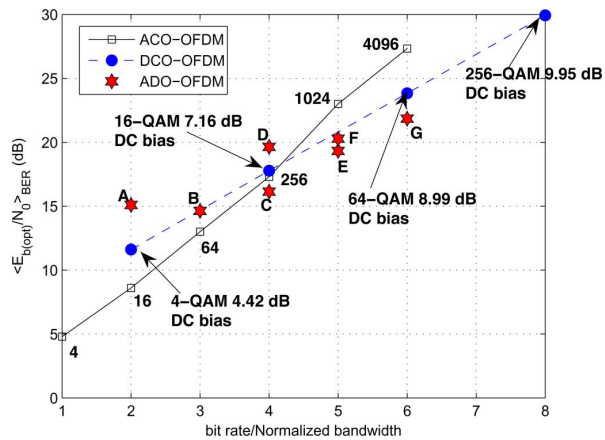

Fig. 10. $\langle E_{\mathrm{b(opt)}}/N_0\rangle_{\mathrm{BER}}$ versus the bit rate/normalized bandwidth per bit rate is shown for ACO-OFDM and ADO-OFDM. Minimum possible $\langle E_{\mathrm{b(opt)}}/N_0\rangle_{\mathrm{BER}}$ for each constellation of DCO-OFDM along with the DC bias are also shown..

ACO-OFDM, the DC-bias level of DCO-OFDM and the constellations that are sent on odd and even subcarriers.

For ADO-OFDM, $E_{\mathrm{b(opt)}}/N_0$ is given by $E\{x'(t)\}/b_{\mathrm{ADO}}N_0$, where the bit rate of ADO-OFDM is given by b_{ADO}. In order to get normalized $E_{\mathrm{b(opt)}}/N_0$ for ADO-OFDM, the average optical power component, $E\{x'(t)\}$, is set to unity. Similarly to ACO-OFDM and DCO-OFDM, the normalized bandwidth of ADO-OFDM is given by $1 + 2/N$. Since, half of the subcarriers in ADO-OFDM carry ACO-OFDM symbols with a QAM constellation of size M_{ACO} and the other half carry DCO-OFDM symbols with a QAM constellation of size M_{DCO}, the average bit rate of ADO-OFDM is given by $(\log_2 M_{\mathrm{ACO}} + \log_2 M_{\mathrm{DCO}})/2$. Therefore, for ADO-OFDM the bit rate/normalized bandwidth is given by $((\log_2 M_{\mathrm{ACO}} + \log_2 M_{\mathrm{DCO}})/2)/(1 + 2/N)$. For example, for an ADO-OFDM scheme that transmits 256-QAM ACO-OFDM and 4-QAM DCO-OFDM. The bit rate/normalized bandwidth rate will be 5.

To determine the best choice of parameters for a given bit rate/normalized bandwidth, a number of simulations were performed. ACO-OFDM, DCO-OFDM and ADO-OFDM with 1024 subcarriers were considered in the simulations and a CP was not used.

Fig. 8, is for the case where 4-QAM with a DC bias of 7 dB is used for the DCO-OFDM component, and the proportion of optical power allocated to the ACO-OFDM component is varied from 0.1 to 0.9. The four plots show the results for 4-QAM, 16-QAM, 64-QAM and 256-QAM constellations on the ACO-OFDM subcarriers. The total optical power of the ADO-OFDM schemes is normalized to unity. The plots show the $\langle E_{\mathrm{b(opt)}}/N_0\rangle_{\mathrm{BER}}$ versus the proportion of optical power on ACO-OFDM. When the ACO-OFDM constellation is 4-QAM the proportion of optical power on the ACO-OFDM subcarriers required to achieve the minimum $\langle E_{\mathrm{b(opt)}}/N_0\rangle_{\mathrm{BER}}$ is 0.2. For larger constellations such as 256-QAM the minimum $\langle E_{\mathrm{b(opt)}}/N_0\rangle_{\mathrm{BER}}$ is achieved when a larger proportion of the optical power is assigned to ACO-OFDM. This is because larger constellation requires a higher SNR for a given BER.

Fig. 9 shows the effect of varying the DC bias level on the DCO-OFDM component and the proportion of optical power allocated to ACO-OFDM. The constellation sizes were kept constant with 4-QAM for DCO-OFDM, and 256-QAM for ACO-OFDM. For all cases the minima of $\langle E_{\mathrm{b(opt)}}/N_0\rangle_{\mathrm{BER}}$ is seen when the optical power on ACO-OFDM is 0.7. This power level is the same as the proportion of optical power on ACO-OFDM required by the same ADO-OFDM scheme in Fig. 8 to achieve minimum $\langle E_{\mathrm{b(opt)}}/N_0\rangle_{\mathrm{BER}}$. Therefore, for a particular ADO-OFDM scheme, the proportion of optical power that is required to be on the ACO-OFDM to obtain the minimum $\langle E_{\mathrm{b(opt)}}/N_0\rangle_{\mathrm{BER}}$, is independent of the DC bias level. However, with increasing DC bias the value of minimum $\langle E_{\mathrm{b(opt)}}/N_0\rangle_{\mathrm{BER}}$ increases. The minimum $\langle E_{\mathrm{b(opt)}}/N_0\rangle_{\mathrm{BER}}$ is achieved at a DC bias of 3.9 dB for this particular case, as seen in Fig. 9.

In Fig. 10, $\langle E_{\mathrm{b(opt)}}/N_0\rangle_{\mathrm{BER}}$ versus the bit rate/normalized bandwidth is shown. Graphs are plotted for ACO-OFDM, for DCO-OFDM bias with the lowest $\langle E_{\mathrm{b(opt)}}/N_0\rangle_{\mathrm{BER}}$, and for a range of ADO-OFDM schemes. For fair comparison of the

TABLE II
ADO-OFDM CONSTELLATIONS USED IN FIG. 10

A	ACO-OFDM 4-QAM, DCO-OFDM 4-QAM, DC bias= 5.5 dB, ACO-OFDM power =0.2
B	ACO-OFDM 16-QAM, DCO-OFDM 4-QAM, DC bias=5.1dB, ACO power =0.4
C	ACO-OFDM 64 QAM, DCO-OFDM 4 QAM, DC bias= 4.3dB, ACO power=0.6
D	ACO-OFDM 16-QAM, DCO-OFDM 16-QAM, DC bias=7.3dB, ACO power=0.2
E	ACO-OFDM 256-QAM, DCO-OFDM 4-QAM, DC bias=3.9dB, ACO power=0.7
F	ACO-OFDM 64-QAM, DCO-OFDM 16-QAM, DC bias=6.6dB, ACO power=0.4
G	ACO-OFDM 256-QAM, DCO-OFDM 16-QAM, DC bias=6.46dB, ACO power=0.5

three modulation schemes the average optical power of each is set to unity. As the ADO-OFDM signal is made up of the two parts, ACO-OFDM and DCO-OFDM, the proportion of power on the two parts can be varied while keeping the power of the transmitted ADO-OFDM signal unity. Table II shows the parameters used for the ADO-OFDM schemes plotted in Fig. 10. The proportion of optical power on ACO-OFDM and DC bias level on DCO-OFDM were varied to achieve the minimum $\left\langle E_{\mathrm{b(opt)}}/N_0\right\rangle_{\mathrm{BER}}$. The values for ACO-OFDM power, which is the proportion of optical power on ACO-OFDM, and DC bias were determined by running extensive simulations of the type shown in Fig. 8 and Fig. 9. For example, point E represents a case when 256 QAM is sent on the ACO-OFDM subcarriers and 4-QAM is sent on the DCO-OFDM subcarriers. The power on the ACO-OFDM component is set to 0.7 of the total optical power, and the DC bias level for the DCO-OFDM component is set to 3.9 dB.

For a bit rate/normalized bandwidth of 4, 5 and 6, ADO-OFDM gives lower $\left\langle E_{\mathrm{b(opt)}}/N_0\right\rangle_{\mathrm{BER}}$ than the conventional schemes ACO-OFDM and DCO-OFDM. The $\left\langle E_{\mathrm{b(opt)}}/N_0\right\rangle_{\mathrm{BER}}$ for point E is 3.68 dB lower than what is required for 1024-QAM ACO-OFDM. For point G, $\left\langle E_{\mathrm{b(opt)}}/N_0\right\rangle_{\mathrm{BER}}$ is 21.85 dB, this is almost 1.9 dB less than 64-QAM DCO-OFDM sent with a 8.99 dB DC bias level.

ADO-OFDM gives better overall performance than either ACO-OFDM and DCO-OFDM for some bit rates/normalized bandwidths. This is because in these cases the combination of the improved spectral efficiency relative to ACO-OFDM and the improved optical power efficiency relative to DCO-OFDM more than compensates for the 3 dB increase in AWGN on the DCO-OFDM component of ADO-OFDM caused by the interference cancellation process described in Section II-D.

IV. CONCLUSION

In this paper, ADO-OFDM, a recently developed modulation scheme for IM/DD systems, is analyzed and the performance of ADO-OFDM compared with ACO-OFDM and DCO-OFDM. In ADO-OFDM the odd subcarriers are modulated using ACO-OFDM and the even subcarriers are modulated using DCO-OFDM. The performance of ADO-OFDM depends on a number of parameters, including the proportion of optical power allocated to the ACO-OFDM and DCO-OFDM components, the constellations used on each component, and the DC bias used for the DCO-OFDM component. The optimal values are found for a number of configurations and it is shown that in a number of cases ADO-OFDM requires less optical power than existing schemes.

APPENDIX

Equation (27) can be written as

$$\begin{aligned} f_{x'(t)}(z) = &\frac{1}{2}\delta(z)Q\left(\frac{B_{\mathrm{DC}}}{\sigma_{\mathrm{D}}}\right) \\ &+\frac{1}{\sqrt{2\pi}\sigma_{\mathrm{A}}}\exp\left[\frac{-z^2}{2\sigma_{\mathrm{A}}^2}\right]u(z)Q\left(\frac{B_{\mathrm{DC}}}{\sigma_{\mathrm{D}}}\right) \\ &+\frac{1}{2\sqrt{2\pi}\sigma_{\mathrm{D}}}\exp\left(\frac{-(z-B_{\mathrm{DC}})^2}{2\sigma_{\mathrm{D}}^2}\right)u(z) \\ &+\underbrace{\int_0^x \frac{1}{2\pi\sigma_{\mathrm{A}}\sigma_{\mathrm{D}}}\exp\left(\frac{(z-\lambda)}{-2\sigma_{\mathrm{A}}^2}+\frac{(\lambda-B_{\mathrm{DC}})^2}{-2\sigma_{\mathrm{D}}^2}\right)d\lambda}_{B}. \end{aligned}$$

To simplify B the following two formulae are used [18]

$$\int_u^\infty \exp\left(\frac{-x^2}{4\beta}-\gamma x\right)dx = \sqrt{\pi\beta}\exp(\beta\gamma^2)Q \times\left(\gamma\sqrt{\beta}+\frac{u}{2\sqrt{\beta}}\right)[\mathrm{Re}\beta>0]$$

and

$$\int_0^\infty \exp\left(\frac{-x^2}{4\beta}-\gamma x\right)dx=\sqrt{\pi\beta}\exp(\beta\gamma^2)Q(\gamma\sqrt{\beta})[\mathrm{Re}\beta>0]$$

Therefore,

$$\int_0^u \exp\left(\frac{-x^2}{4\beta}-\gamma x\right)dx = \int_0^\infty \exp\left(\frac{-x^2}{4\beta}-\gamma x\right)dx - \int_u^\infty \exp\left(\frac{-x^2}{4\beta}-\gamma x\right)dx,$$

which simplifies to

$$\int_0^u \exp\left(\frac{-x^2}{4\beta}-\gamma x\right)dx = \sqrt{\pi\beta}\exp(\beta\gamma^2) \times\left[Q(\gamma\sqrt{\beta})-Q\left(\gamma\sqrt{\beta}+\frac{u}{2\sqrt{\beta}}\right)\right].$$

REFERENCES

[1] H. Elgala, R. Mesleh, and H. Haas, "Practical considerations for indoor wireless optical system implementation using OFDM," in *Pro. ConTEL*, Zagreb, Croatia, 2009, pp. 25–30.

[2] J. Armstrong and B. J. C. Schmidt, "Comparison of asymmetrically clipped optical OFDM and DC-biased optical OFDM in AWGN," *IEEE Commun. Lett.*, vol. 12, pp. 343–345, 2008.

[3] J. Armstrong, "OFDM for optical communications," *J. Lightw. Technol.*, vol. 27, pp. 189–204, 2009.

[4] J. Armstrong and A. J. Lowery, "Power efficient optical OFDM," *Electron. Lett.*, vol. 42, pp. 370–372, 2006.

[5] J. M. Kahn and J. R. Barry, "Wireless infrared communications," *Proc. IEEE*, vol. 85, p. 1997, 265–298.

[6] K. Asadzadeh, A. Dabbo, and S. Hranilovic, "Receiver design for asymmetrically clipped optical OFDM," in *Proc. IEEE GLOBECOM OWC Workshop*, Houston, TX, USA, 2011.
[7] S. C. J. Lee, F. Breyer, D. Cardenas, S. Randel, and A. M. J. Koonen, "Real-time gigabit DMT transmission over plastic optical fibre," *Electron. Lett.*, vol. 45, pp. 1342–1343, 2009.
[8] K. Asadzadeh, A. A. Farid, and S. Hranilovic, "Spectrally factorized optical OFDM," in *Proc. 12th Can. Workshop Inf. Theory (CWIT)*, Kelowna, BC, Canada, 2011, pp. 102–105.
[9] L. Chen, B. Krongold, and J. Evans, "Diversity combining for asymmetrically clipped optical OFDM in IM/DD channels," in *Proc. IEEE GLOBECOM*, Honolulu, HI, USA, Dec. 2009, pp. 1–6.
[10] S. D. Dissanayake and J. Armstrong, "Novel techniques for combating DC-Offset in Diversity combined ACO-OFDM," *IEEE Commun. Lett.*, vol. 15, pp. 1237–1239, 2011.
[11] S. D. Dissanayake, J. Armstrong, and S. Hranilovic, "Performance analysis of noise cancellation in a diversity combined ACO-OFDM system," in *Proc. Int. Conf. Transparent Optical Networks (ICTON)*, Warwick, U.K., 2012.
[12] S. D. Dissanayake, K. Panta, and J. Armstrong, "A novel technique to simultaneously transmit ACO-OFDM and DCO-OFDM in IM/DD systems," in *Proc. IEEE GLOBECOM Workshops*, Houston, TX, USA, 2011, pp. 782–786.
[13] J. Armstrong, "Analysis of new and existing methods of reducing intercarrier interference due to carrier frequency offset in OFDM," *IEEE Trans. Commun.*, vol. 47, pp. 365–369, 1999.
[14] C. Liang, B. Krongold, and J. Evans, "Performance analysis for optical OFDM transmission in short-range IM/DD systems," *J. Lightw. Technol.*, vol. 30, pp. 974–983, 2012.
[15] D. J. F. Barros, S. K. Wilson, and J. M. Kahn, "Comparison of orthogonal frequency-division multiplexing and pulse-amplitude modulation in indoor optical wireless links," *IEEE Trans. Communications*, vol. 60, pp. 153–163, 2012.
[16] X. Li, R. Mardling, and J. Armstrong, "Channel capacity of IM/DD optical communication systems and of ACO-OFDM," in *Proc. IEEE Int. Conf. Communications*, Glasgow, U.K., 2007, pp. 2128–2133.
[17] J. Armstrong, B. J. C. Schmidt, D. Kalra, H. A. Suraweera, and A. J. Lowery, "Performance of asymmetrically clipped optical OFDM in AWGN for an intensity modulated direct detection system," in *Proc. IEEE GLOBECOM 2006*, San Francisco, CA, USA, 2006, pp. 1–5.
[18] I. Gradshteyn and I. Ryzhik*, Table of Integrals, Series and Products*, 6th ed. New York, NY, USA: Academic, 2000.

Sarangi Devasmitha Dissanayake (S'11) received the B.Sc. degree (with first class honors) in electronics and telecommunication engineering from the University of Moratuwa, Sri Lanka, in 2007. She is currently working toward the Ph.D. degree at the Department of Electrical and Computer Systems Engineering, Monash University, Clayton, Australia.

From 2007 to 2009 she worked at Dialog Telekom PLC, Colombo, Sri Lanka as a Telecommunication Engineer. In 2010, she was selected as the Australia/New Zealand Google Anita Borg Memorial Scholar which is awarded to an outstanding female student studying an ICT related course in a university in Australia/New Zealand. Her research interests include orthogonal frequency division multiplexing, optical wireless communication and wireless communication for vehicular networks.

Jean Armstrong (M'89–SM'06) received the B.Sc. (first class honors) in electrical engineering from the University of Edinburgh, U.K., in 1974, the M.Sc. degree in digital techniques from Heriot-Watt University, Edinburgh, U.K., in 1980, and the Ph.D. degree in digital communications from Monash University, Melbourne, Australia, in 1993.

From 1974–1977 she worked as a Design Engineer at Hewlett-Packard Ltd., Scotland. In 1977 she was appointed Lecturer in Electrical Engineering at the University of Melbourne, Australia. Since 1977 she has held a range of academic positions at the University of Melbourne, MonashUniversity and La Trobe University. She is currently a Professor at Monash University Her research interests include digital communications, engineering education, and women in engineering. Most of her recent research has been on Orthogonal Frequency Division Multiplexing (OFDM) and she has published many very highly cited papers and has six fully commercialized patents in this field. Her earlier OFDM work was on RF wireless applications, but in 2005 she recognized the potential for applying OFDM to optical communications.

Prof. Armstrong has been the recipient of numerous awards including induction into the Victorian Honour Roll of Women, the Peter Doherty for the best commercialization opportunity in Australia in 2006 (joint winner), Institution of Engineers, Australia, Engineering 2000 Award, Zonta International Amelia Earhart Fellowship and Caroline Haslett Memorial Scholarship. She is a Fellow of the Institution of Engineers Australia. She is currently a member of the Australian Research Council (ARC) College of Experts.